Clinical Radiology 77 (2022) 96–103

Contents lists available at ScienceDirect

Clinical Radiology

journal homepage: www.clinicalradiologyonline.net

Automatic detection of Crohn's disease using quantified motility in magnetic resonance enterography: initial experiences

A. Arkko [a,*], T. Kaseva [a], E. Salli [a], T. Mäkelä [a,b], S. Savolainen [a,b], M. Kangasniemi [a]

[a] HUS Medical Imaging Center, Radiology, Helsinki University Hospital and University of Helsinki, P.O. Box 340, FI-00290, Helsinki, Finland
[b] Department of Physics, University of Helsinki, P.O. Box 64, FI-00014, Helsinki, Finland

ARTICLE INFORMATION

Article history:
Received 2 July 2021
Accepted 6 October 2021

AIM: To report initial experiences of automatic detection of Crohn's disease (CD) using quantified motility in magnetic resonance enterography (MRE).

MATERIALS AND METHODS: From 302 patients, three datasets with roughly equal proportions of CD and non-CD cases with various illnesses were drawn for testing and neural network training and validation. All datasets had unique MRE parameter configurations and were performed in free breathing. Nine neural networks were devised for automatic generation of three different regions of interests (ROI): small bowel, all bowel, and non-bowel. Additionally, a full-image ROI was tested. The motility in an MRE series was quantified via a registration procedure, which, accompanied with given ROIs, resulted in three motility indices (MI). A subset of the indices was used as an input for a binary logistic regression classifier, which predicted whether the MRE series represented CD.

RESULTS: The highest mean area under the curve (AUC) score, 0.78, was reached using the full-image ROI and with the dataset with the highest cine series length. The best AUC scores for the other two datasets were only 0.54 and 0.49.

CONCLUSION: The automatic system was able to detect CD in the group of MRE studies with lower temporal resolution and longer cine series showing potential in primary bowel disorder diagnostics. Larger ROI selections and utilising all available cine series for motility registration yielded slight performance improvements.

Introduction

Inflammatory bowel diseases, consisting of Crohn's disease (CD) and ulcerative colitis (UC) continue to present a burgeoning health concern.[1] In CD, magnetic resonance enterography (MRE) is often employed to assess for disease extent and severity and less often in primary diagnostics.

* Guarantor and correspondent: A. Arkko, HUS Medical Imaging Center, Radiology, Helsinki University Hospital and University of Helsinki, P.O. Box 340, FI-00290, Helsinki, Finland. Tel.: +358401865799.
E-mail address: anssi.arkko@hus.fi (A. Arkko).

https://doi.org/10.1016/j.crad.2021.10.006

Dynamic, or "cine", technique in MRE can be used to detect changes in bowel motility, which in addition to focal changes in markedly ill bowel segments, has been suggested to decrease even in portions of bowel that show no apparent indicators of illness.[2] Aberrations in motility also correlate with biomarkers of inflammation and symptoms.[3–5] A general decrease in bowel motility and its variance may therefore indicate underlying disease in otherwise healthy-looking intestine.[3]

Established methodology regarding bowel motility quantification, demonstrated, for example, by Odille *et al.*[6] or Menys *et al.*,[7] include using demons algorithms for motility registration[8,9] and the use of Jacobian determinants computed from deformation fields as a surrogate measure for contractions and expansions of a target area.[10] Traditionally, MRE cine images have been obtained in breath-hold, simplifying motility registration, although free-breathing techniques have also been explored with promising results.[7,11–14] Free breathing enables longer MRE series, which could be beneficial in observing bowel motility.[15] Additionally, although cine images are obtained from several different coronal planes, only one of these planes is often selected for motility computation.[11,15–18]

To date and to the authors' knowledge, even the most automated applications for quantified motility-based detection systems for bowel disease have necessitated some manual effort.[4,6,10–12,19,20] Tools requiring hand-drawn annotations may interfere with clinical workflow, which has prompted interest in the development of a fully automated system. Such a system could be integrated into existing practice, thereby aiding primary diagnostics in bowel disorders where CD is suspected, or indeed, when CD has not even been considered.

The present study investigated the viability of automatic detection of CD in a diverse set of patients with various other illnesses under routine clinical investigations. A detection system was devised based on converting bowel motility into indices combining several techniques previously established in the literature but including deep learning-generated regions-of-interest (ROIs) and the use of multiple cine series obtained from different coronal positions. Different ROIs and motility index selections were evaluated in three datasets with varying MRE imaging parameters to devise the optimal preferences for the method. The goal was to develop the basis for a tool for automatically suggesting the probability of CD from MRE in any patient undergoing initial bowel disorder investigations.

Materials and methods

Patients and datasets

Data from 369 MRE studies conducted in two centres in the Helsinki University Hospital district between March 2013 and 2020 were collected retrospectively. The studies were performed on two 1.5 T Avanto^{fit} and one 3 T Verio scanner by Siemens Healthineers (Erlangen, Germany). The university hospital ethical committee approved this retrospective work and patients' informed consent was waived.

For the purposes of this work, only the free-breathing cine MRE series were utilised from all coronal positions imaged in a single session during each study. These sets are referred to as the "*cine sets*". Using these cine sets, three homogeneous datasets were defined through the following process as illustrated in Fig 1. First, only cine sets from patients with confirmed CD or excluded CD diagnosis were included resulting in the exclusion of 12 cine sets. CD was confirmed when stated in the gastroenterology report based on imaging and laboratory studies, endoscopy, and biopsy. Other bowel disorders were included to assess the possibility of detecting CD in a realistic setting. The second inclusion criteria outlined that the cine MRE repetition times were either 425.5, 193.1, or 143.1 milliseconds. These correspond to approximate temporal resolutions of 2, 5, and 7 frames/s, respectively. After the resulting 36 cine set exclusions, three groups were constructed. The three repetition times were chosen to improve the variability of the experiments, and because only the study groups with these repetition times were numerous enough for reasonable experiments. Thirdly, only one cine set for each patient was allowed. Where multiple cine sets were available, inclusion was prioritised in the smallest 424.5 milliseconds repetition time group, and then the oldest study. After 17 exclusions, the final datasets 1, 2, and 3 were formed. The dataset demographics and imaging parameters are presented in Table 1 and the composition of the non-CD group in Table 2.

Imaging protocol

Standardised magnetic resonance imaging (MRI) protocols are followed in the hospital district imaging centres concurrently, but the number of coronal planes and cine series lengths varied between 2013 and 2020. The coronal planes were selected by MRI technicians to cover the maximal bowel area in the allotted time and not otherwise targeted. All were conducted in free breathing. Prior to MRE, an easily digestible diet was permitted, and on the previous day two tablets of laxative bisacodyl were applied. A fast

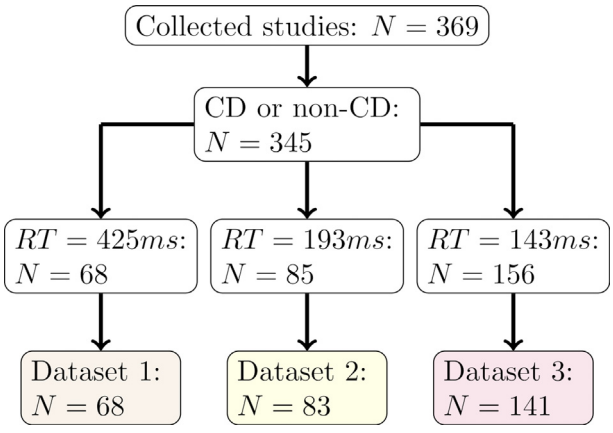

Figure 1 Exclusion criteria flowchart. CD, Crohn's disease. RT, Repetition time (time resolution).

Table 1
Demographics and imaging parameters of datasets 1, 2, and 3.

Imaging parameters	Dataset		
	1	2	3
No. of patients	72	85	145
Non-CD percentage	43%	53%	53%
Female percentage	53%	53%	63%
Mean age, years (SD)	45 (16.5)	39 (14.4)	41 (16.4)
Field strength	1.5T	3T	1.5T
Sequence type	T2 True FISP	T2 True FISP	T2 True FISP
Echo time, ms	1.68	1.27	1.15
Repetition time, ms	425.45	193.12	143.1
Series length, s	16.6	7.4	5.5
Section thickness, mm	10	10	10
Image pixel size, mm	0.74 × 0.74	1.56 × 1.56	1.52 × 1.52
Acquisition matrix	256 × 257	256 × 204	224 × 181
Flip angle range	60°	32–40°	48–67°
Average no. of cine series per patient	3	8	6

True FISP, true fast imaging with steady state free precession; CD, Crohn's disease.

was imposed, but drinking allowed up until 4 h before imaging. Starting 45 minutes before imaging, 1,500 ml of mannitol contrast agent was applied gradually either by ingestion or nasojejunal catheter. The use of the nasojejunal catheter was phased out between the years 2013 and 2015 after which it was used only when oral intake was difficult. Intravenous gadolinium and antimuscarinic scopolamine or glucagon were administered after cine imaging.

Manual segmentations

ROI types for motility estimation were: (1) small bowel = SB-ROI, (2) both small bowel and colon, i.e., all bowel = AB-ROI, (3) inverse of the AB-ROI, i.e., non-bowel = NB-ROI, and (4) full image area = FI-ROI. The NB-ROI was used as a check for spurious effects emanating outside the bowel. Examples of ROI categories are presented in Fig 2. To prepare training data for deep learning, subsets of these ROIs were segmented manually and semi-automatically.

Table 2
Imaging indications and/or confirmed diagnoses in the non-Crohn's disease cases.

Imaging indication/diagnosis	No. of cases
CD initially suspected, no confirmed bowel diagnosis	44
Unresolved abdominal symptoms, CD suspicion not stated and no confirmed bowel diagnosis	28
Irritable bowel syndrome	25
Tumour, suspected or follow-up	19
Ulcerative colitis	10
Unresolved intestinal obstruction	9
Microscopic anaemia	8
Familial adenomatous polyposis	6
Diabetic gastroparesis	2
Miscellaneous[a]	7

CD, Crohn's disease.
[a] Confirmation of incidental findings in other studies, one case of caecal tuberculosis, one case of dientamoeba.

The AB-ROIs were annotated on datasets 2 and 3. The annotators were a radiologist with 6 years of experience and a specialist researcher with 4 years of experience in AI research. A total of 1,214 coronal sections of cine series were segmented. One week was allocated for this process. The number of segmented sections differed between cine sets but at least one section was segmented per set to increase the variation in the data.

All the coronal cine series in dataset 1, a total number of 8,268 sections, were fully segmented for the SB-ROIs. This process was performed with help from a previously developed in-house U-Net network designed for AB-ROI segmentation and the registration method discussed in detail in the Electronic Supplementary Material. Small imperfections in the SB-ROIs, such as shown in Fig 2, were considered acceptable after the correction operation.

System for CD detection

A CD detection system was developed, which takes MRE series as an input and produces a probability of the disease. The system was based on quantification of bowel motility followed by binary classification. The system and its configurations are briefly described below and demonstrated graphically in Fig 3. Detailed explanations for the processes of ROI generation, neural network training, motility

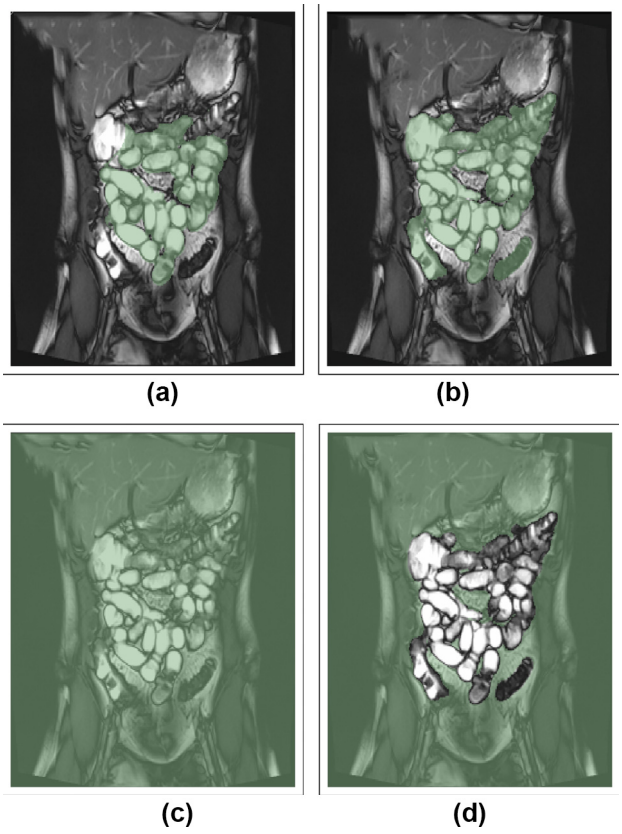

Figure 2 Examples of ROI categories marked with green colour. (a) SB-ROI containing only the small bowel, (b) AB-ROI containing colon in addition to small bowel, (c) FI-ROI, and (d) NB-ROI, the inverse of AB-ROI, i.e., the area outside bowel.

quantification, and binary classification are provided in the Electronic Supplementary Material.

First, all the coronal cine MRE series of the cine sets were registered to their mid-time-point image using a diffeomorphic demons algorithm,[8] which expands on the original Thirion's demons[9] and is a variation of an optical-flow method,[21] implemented into Insight Toolkit (ITK).[22] The demons method is used to estimate displacement fields between images and their reference point, which corresponds to motion in the case of moving objects such as the bowel. Then, the pixel-wise standard deviations of the Jacobian determinants were computed over time. Motility maps were formed by masking the standard deviation maps with a chosen ROI type. Four different ROI types were considered in these experiments.

A total of nine U-Nets were trained for generation of the SB-, AB- and NB-ROIs. All the U-Nets had the same model architecture, similar to that proposed by Ronneberger *et al.*[23] The input dimensions were 256 × 256 pixels, and all training and testing data were resized to match this requirement. Eight of the U-Nets were trained for the small-bowel segmentation via eightfold cross-validation using the manually segmented sections of dataset 1. The U-Nets segmented their test sets which were separated from the training data and which combined all the cine series in dataset 1. The last U-Net was trained for all-bowel segmentation using the manually segmented sections in datasets 2 and 3. It was used to segment the cine series of dataset 1.

Three motility indices were computed from the motility maps: MI_1, which was an average over all motility maps, MI_2, an average over the most motile motility map and MI_3, an average over the motility map with the largest ROI. Finally, a subset of the motility indices was fed to a binary logistic regression classifier, which predicted the probability of CD of the patient. These subsets were denoted as either MI_i, $MI_{i,j}$ or $MI_{i,j,k}$ where i, j and k were either 1, 2 or 3. Seven different motility index subsets were considered and as the number of ROI types was four the proposed system had 28 different configurations. In Fig 3, the system configuration with $M_{1,2,3}$ subset and AB-ROI is illustrated.

Motility quantification was performed on all cine sets in the datasets 1, 2, and 3. With dataset 1, the motility indices were computed using all four ROI types. With datasets 2 and 3, only full image ROI was used. The reason for this is elaborated in the Discussion section.

Evaluation

The results of the seven classifier models on the datasets were summarised using cross-validation and receiver operating characteristic (ROC) curves and the areas under these curves (AUC). Consider one of the motility index sets discussed in the end of "Quantification of motility" and one of the seven classifier models. First, the set was divided into four equal or close to equal-sized folds. The classifier model was then trained four times, using each time different fold as a test and the rest as a training set. During training, class weights were adjusted automatically to be inversely proportional to class frequencies. The fourfold cross-validation was performed 1,000 times with shuffling the motility index set each time prior to the training. As a result, 4,000 prediction result sets were obtained with each set consisting of CD probabilities of each sample in the set's corresponding test fold. Mean ROC and AUC scores were then computed over these sets. The evaluation procedure was replicated for each model and motility index set, resulting in 28 ROC AUC scores for dataset 1, seven for dataset 2, and seven for dataset 3.

The segmentation accuracy was assessed using Dice score[24] that measures the overlap between manual and automatic segmentation. The seven U-Nets that trained for the small bowel segmentation were evaluated using their test sets. Effectively, the test sets consisted of all the studies in dataset 1. The Dice score for the U-Net, which produced AB-ROI segmentations, was obtained using the model's validation set since dataset 1 had no reference all bowel segmentations.

Results

The average AUC scores for the different CD detection system configurations are shown in Table 3. ROC curves with all ROI types and four different motility index sets are visualised in Fig 4. The scores on datasets 2 and 3 were in average 30% lower than on dataset 1. The best performing motility index combinations consisted either of MI_1 or MI_2, which describe the motility over all the cine series and over the one with the most motility, respectively. In addition, the use of $M_{1,3}$ benefitted the configuration with SB-ROI the most. The highest mean AUC score, 0.78, was obtained on dataset 1 with FI-ROI. The second-best result of 0.76 was obtained with SB-ROIs whereas the configurations using AB-ROIs and NB-ROIs reached 0.70.

The average Dice score of the small bowel segmentations over dataset 1 was 0.82 and the standard deviation 0.12; however, the results on some of the cine sets were especially poor due to high variation in the images. For instance, if five cine sets with the lowest Dice scores were excluded, the average score reached 0.84. The all-bowel segmentations on the validation set of the cine sets discussed in section ROI generation with U-Nets achieved 0.82 average Dice score and the standard deviation was 0.06.

Discussion

The aim of the present study was to investigate the viability of automatically recognising the probability of CD in dynamic MRE images obtained without breath-hold and to suggest preferences for the technique. Retrospectively collected cine MRE series were divided into three homogeneous datasets. Imaging parameters, such as repetition time (i.e., temporal resolution), differed between the sets. A recognition system was designed, which combined established techniques and U-Net for automatic ROI generation, and the added potential of combining information from all the coronal cine series of an MRE study was investigated.

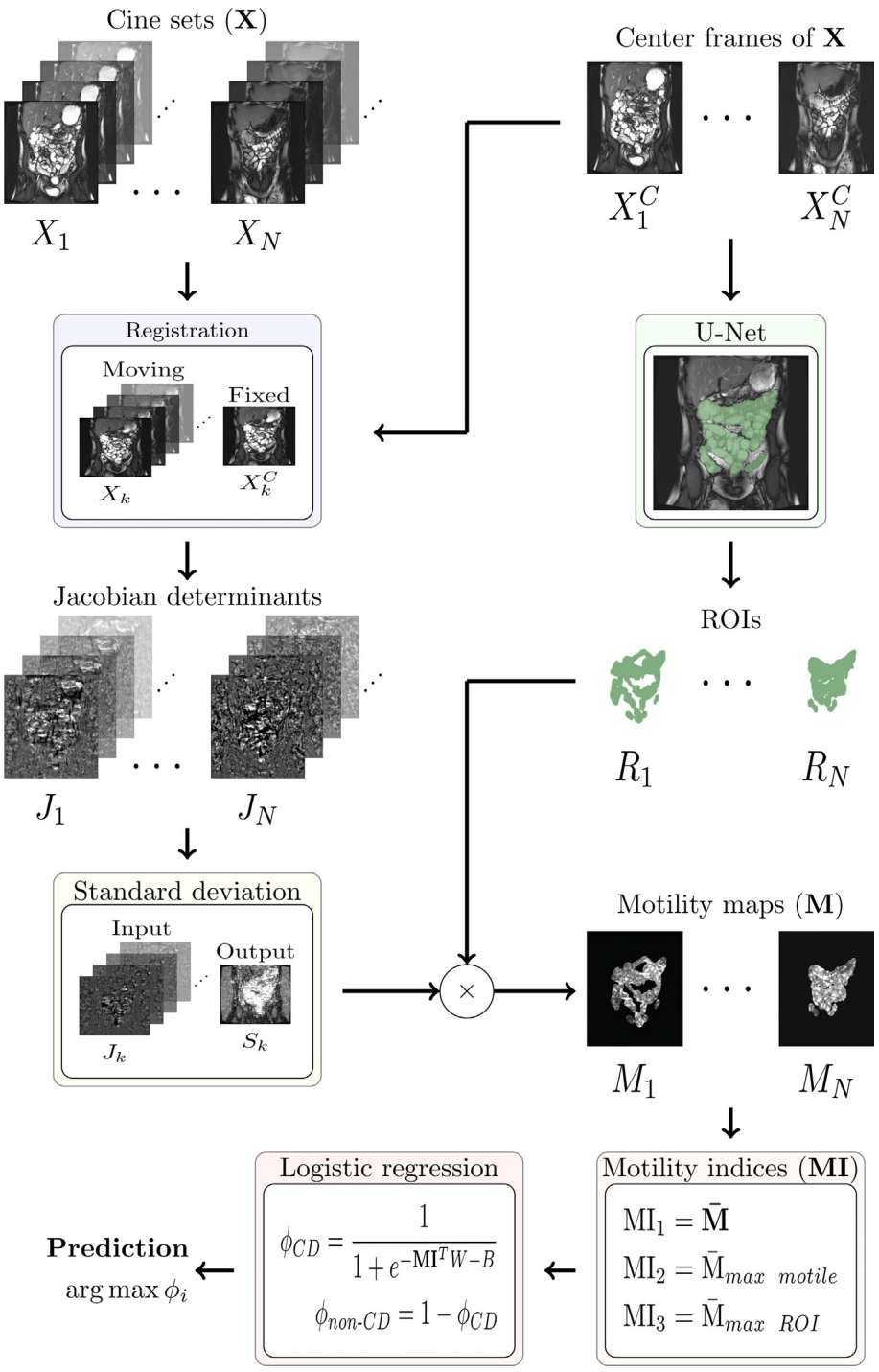

Figure 3 System for CD detection, graphical summary. ROI, region of interest, CD, Crohn's disease.

The technical novelties of the present work are as follows. Firstly, fully automatic ROI selection was investigated. ROIs for the small bowel, small bowel, colon, and non-bowel were generated using U-Nets. Although neural networks have been used before for small bowel segmentation in a motility quantification scheme,[25,26] in these works, ROI generation has been semi-automatic. Furthermore, to the best of the authors' knowledge, the present study is the first to investigate whether the motility in the regions outside the small bowel contributes to CD detection. Secondly, the input of the proposed CD detection system consisted of a varying number of cine MRE series. The use of only a single MRE series for motility assessment has been dominant in the related literature[7,15,17,19,20] and some studies have reported it as a limitation.[19,20]

The main result of this paper was that the system could detect CD from cine MRE series with relatively high confidence in dataset 1 but not in datasets 2 or 3. The best mean

Table 3
Mean AUC scores and their standard deviations of the CD detection system configurations.

	ROI	MI_1	MI_2	MI_3	$MI_{1,2}$	$MI_{1,3}$	$MI_{2,3}$	$MI_{1,2,3}$
Dataset 1	AB	0.70 ± 0.12	0.69 ± 0.12	0.64 ± 0.13	0.68 ± 0.12	0.68 ± 0.12	0.68 ± 0.12	0.67 ± 0.12
	FI	0.78 ± 0.10	0.76 ± 0.11	0.71 ± 0.12	0.76 ± 0.11	0.76 ± 0.11	0.76 ± 0.11	0.75 ± 0.11
	SB	0.72 ± 0.12	0.73 ± 0.11	0.59 ± 0.13	0.72 ± 0.11	0.76 ± 0.11	0.72 ± 0.11	0.75 ± 0.11
	NB	0.70 ± 0.12	0.64 ± 0.13	0.65 ± 0.12	0.68 ± 0.12	0.68 ± 0.12	0.64 ± 0.13	0.66 ± 0.12
Dataset 2	FI	0.49 ± 0.12	0.54 ± 0.12	0.42 ± 0.08	0.52 ± 0.12	0.49 ± 0.12	0.53 ± 0.11	0.49 ± 0.11
Dataset 3	FI	0.49 ± 0.09	0.48 ± 0.08	0.44 ± 0.06	0.44 ± 0.08	0.48 ± 0.08	0.46 ± 0.08	0.45 ± 0.08

ROI, region of interest. AB, all bowel, FI, full image, SB, small bowel, and NB, non-bowel, inverse of AB. MI_i, $MI_{i,j}$, $MI_{i,j,k}$, describe different motility index input combinations of the seven logistic regression classifier models.

AUC score achieved with datasets 2 and 3 was only 0.54. As illustrated in Table 2, dataset 1 had the highest pixel resolution, the lowest temporal resolution, and considerably longer temporal length in cine MRE series. In particular, the last two factors contributed to the success of CD detection with dataset 1. MRI field strength did not seem a deciding factor as there was little difference between dataset 2 (3T) and dataset 3 (1.5T). Although the average number of cine MRE series per study was the lowest with the best-performing dataset 1, the coronal locations of the series were not targeted on visible signs of disease in the used MRE protocol.

Secondly, the highest mean AUC score of 0.78 was obtained with dataset 1 using the FI-ROI while the best scores with SB-ROI, AB-ROI, and NB-ROI were 0.76, 0.70, and 0.70. One reason for the result might have been the imperfection of the automatically generated ROIs. The score of NB-ROI suggested that motility in the non-bowel region also contributed to the CD detection task. The prominent movement in this region consisted of respiratory motion. One possible theory derived from this is that the present results reflected changes in breathing patterns caused by illness. This is an unlikely explanation in the present setting, as the control group of non-CD patients also comprised patients with varying illnesses. It is plausible that CD-induced motility changes in the bowel could be reflected in the non-bowel regions, such as the mesentery. Jacobian determinants can be considered a surrogate marker for local expansion and contraction, and volume changes in other organs could register as motility. Visual inspections on the motility maps indicated that most of the quantified motility manifested in the bowel regions. As the motility indices were calculated simply as means over the maps, the bowel region contributed heavily to the values of the indices with the FI-ROIs. Nevertheless, respiratory motion affecting the results to some degree cannot be completely ruled out.

SB-ROIs, NB-ROIs, and AB-ROIs were not generated for datasets 2 and 3 as visual inspections revealed that the seven U-Nets trained for small bowel segmentation were incapable of producing reliable segmentations on the datasets. As the best results with dataset 1 were obtained with FI-ROI, the use of only this ROI would be sufficient to summarise the performance of the CD detection system on datasets 2 and 3.

Thirdly, modest detection improvement was observed when motility was quantified using each cine MRE series in the cine set. With dataset 1, the best performing motility index subset was MI_1, which was computed using all motility maps; however, the motility map from which either MI_2 or MI_3 was computed was chosen automatically. If the motility map had been chosen manually by a professional, the results could have differed. As the AUC scores with datasets 2 and 3 were generally low, there was no speculation on the effect of different motility index sets with these datasets.

Finally, the detection of CD in a pool of patients with various illnesses was viable. No healthy control group was or could be established in the present setting. The hypothesis is that CD produces relatively unique, distinguishable changes in overall bowel motility for which the present results offer some initial support. The CD detection capability shown by the present system might have appeared stronger when compared with healthy subjects, but the experiments provide more relevant results from a clinical point of view. A system with the capability of suggesting the probability of CD in a patient with unresolved bowel symptoms as essentially a by-product of MRE could offer a time- and cost-efficient aid in diagnostics. The hope is that detecting motility changes could offer hints of disease even if no other imaging findings are discernible.

Limitations of the present study include issues inherent to the patient data. As CD diagnosis may be delayed, some of the non-CD patients may have presented early bowel motility features of CD during the study period. Intending to avoid quiescent CD masquerading as non-CD in the present analyses, the patient records were investigated for information regarding CD activity; however, the data were found to be unreliable as laboratory and endoscopic studies were not always performed concurrently with MRE and symptoms were recorded inconsistently, as was adherence to patient preparation instructions. For similar reasons, the use of anti-inflammatory drugs was not noted, which did not seem to correlate with motility as tested by Dreja *et al.*, 2020.[15] Additionally, as the cine series were not targeted on any specific bowel regions, the ROI selections could not be compared with specific bowel regions, e.g., the terminal ileum. The effect of age or gender differences between test groups was ruled out in the tests (data not shown).

Based on the present tests, there are two main proposals for future research and clinical practice based on bowel motility: favouring long cine series lengths and repetition times over fine-grain temporal resolution and combining information from each coronal plane to utilise all available

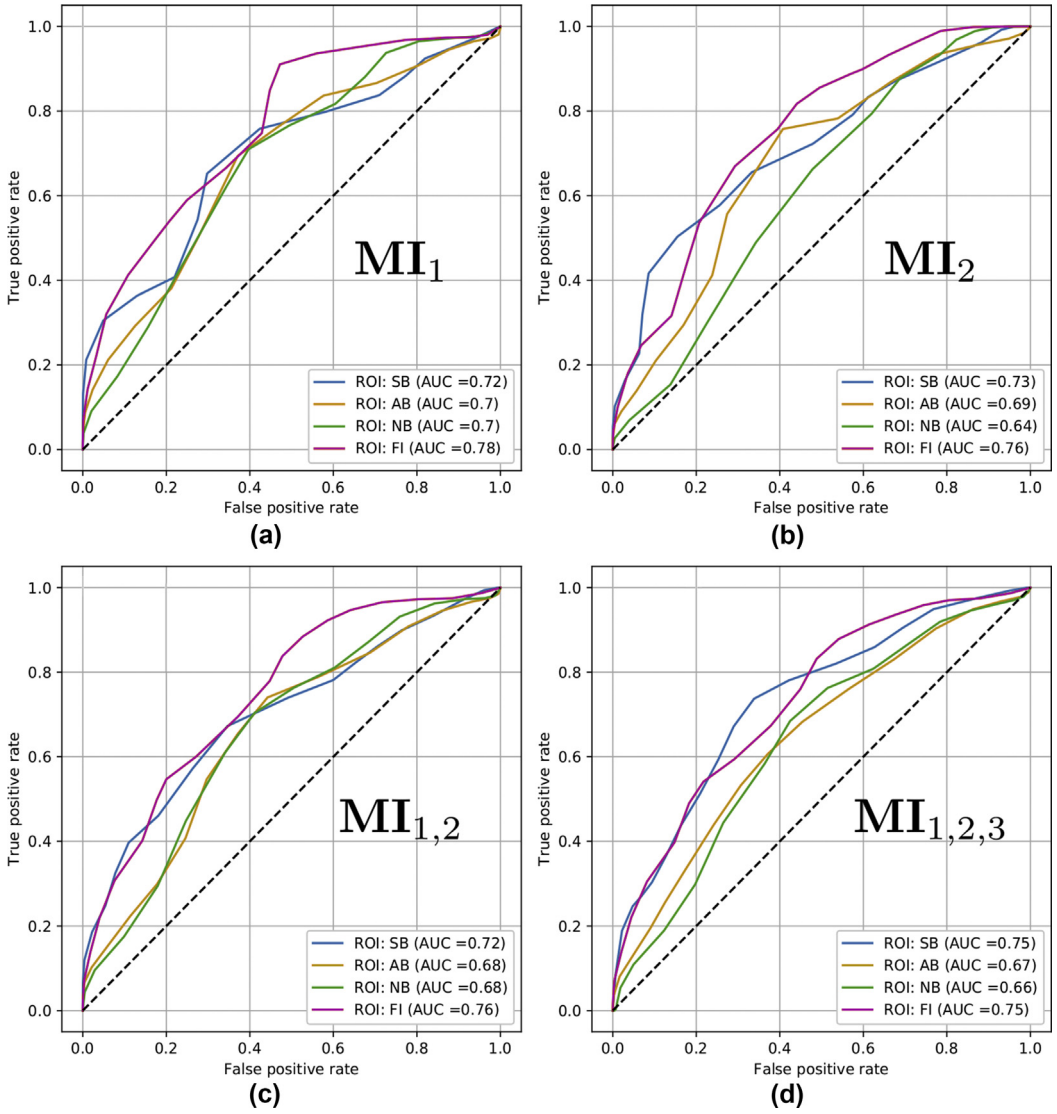

Figure 4 Mean ROC curves of 16 CD detection system configurations on dataset 1. (a) ROC curves of four configurations with the motility index subset fixed to MI_1. (b) To MI_2, (c) to $MI_{1,2}$, and (d) to $MI_{1,2,3}$. ROI, region of interest. SB, the small bowel, AB, both small and large bowel. NB, the inverse of AB. FI, full image. MI_i, $MI_{i,j}$, and $MI_{i,j,k}$ describe different motility index input combinations of the seven logistic regression classifier models. The individual motility indices of these combinations are: MI_1, the mean over all intensity values of all the motility maps, MI_2, the mean over the intensity values of the motility map in which this mean was the highest of all maps, and MI_3 the mean over intensities of the motility map with the largest ROI.

motility data. The former incentivises studies where no breath-hold is used. It may also be beneficial to obtain motility data from more than just the small bowel.

Further studies into the prospects of neural network solutions in CD detection are warranted. For example, machine learning-based analysis of motility maps would be of interest instead of classifying the data according to indices. Pinpointing regional bowel pathology automatically is another possible avenue of investigation. It would also be of great interest to see whether signs of bowel motor dysfunction could be used to predict the onset or flare-up of CD. In addition, improvements in motility registration could be gained with four-dimensional bowel volumetry, a technique demonstrated in one recent project.[15]

In conclusion, the present study describes a system for CD detection in MRE combining established methods for motility quantification with novel approaches. The goal was to produce a system for automatically presenting a clinician with the probability of CD in a patient undergoing MRI for an unidentified bowel disorder. The main finding was that the proposed system could detect CD cases from a pool of patients with various illnesses in dataset 1 but not in datasets 2 and 3. The cine sets of dataset 1 had significantly longer repetition times and series lengths than the sets in datasets 2 and 3. The performance of the system improved when multiple cine MRE series were utilised for motility quantification and with the ROI extended over the full image. The proposed system shows potential as a basis for a

fully automatic aid in primary diagnostics for Crohn's disease.

Conflict of interest

The authors declare no conflict of interest.

Acknowledgements

The authors thank Perttu Laamanen, B.M., for his assistance in drafting the motility registration algorithms in the early stages of this study. This work was supported by the Helsinki University Hospital (S.S.: TYH2019253, K.M.: Y780020122 and A.A.: Y780019034). The funding source did not participate in the preparation of the study or the manuscript.

Appendix A. Supplementary data

Supplementary data to this article can be found online at https://doi.org/10.1016/j.crad.2021.10.006.

References

1. Ng SC, Shi HY, Hamidi N, *et al.* Worldwide incidence and prevalence of inflammatory bowel disease in the 21st century: a systematic review of population-based studies. *Lancet* 2017;**390**:2769–78. https://doi.org/10.1016/S0140-6736(17)32448-0.
2. Khalaf A, Hoad CL, Menys A, *et al.* Gastrointestinal peptides and small-bowel hypomotility are possible causes for fasting and postprandial symptoms in active Crohn's disease. *Am J Clin Nutr* 2020;**111**:131–40. https://doi.org/10.1093/ajcn/nqz240.
3. Menys A, Makanyanga J, Plumb A, *et al.* Aberrant motility in unaffected small bowel is linked to inflammatory burden and patient symptoms in Crohn's disease. *Inflamm Bowel Dis* 2016;**22**:424–32. https://doi.org/10.1097/MIB.0000000000000601.
4. Bickelhaupt S, Froehlich JM, Cattin R, *et al.* Differentiation between active and chronic Crohn's disease using MRI small-bowel motility examinations: initial experience. *Clin Radiol* 2013;**68**:1247–53. https://doi.org/10.1016/j.crad.2013.06.024.
5. Gollifer RM, Menys A, Makanyanga J, *et al.* Relationship between MRI quantified small bowel motility and abdominal symptoms in Crohn's disease patients—a validation study. *Br J Radiol* 2018;**91**:20170914. https://doi.org/10.1259/bjr.20170914.
6. Odille F, Menys A, Ahmed A, *et al.* Quantitative assessment of small bowel motility by nonrigid registration of dynamic MR images. *Magn Reson Med* 2012;**68**:783–93. https://doi.org/10.1002/mrm.23298.
7. Menys A, Hamy V, Makanyanga J, *et al.* Dual registration of abdominal motion for motility assessment in free-breathing data sets acquired using dynamic MRI. *Phys Med Biol* 2014;**59**:4603–19. https://doi.org/10.1088/0031-9155/59/16/4603.
8. Vercauteren T, Pennec X, Perchant A, *et al.* Diffeomorphic demons: efficient non-parametric image registration. *Neuroimage* 2009;**45**:S61–72. https://doi.org/10.1016/j.neuroimage.2008.10.040.
9. Thirion J-P. Image matching as a diffusion process: an analogy with Maxwell's demons. *Med Image Anal* 1998;**2**:243–60. https://doi.org/10.1016/S1361-8415(98)80022-4.
10. Hahnemann M, Nensa F, Kinner S, *et al.* Improved detection of inflammatory bowel disease by additional automated motility analysis in magnetic resonance imaging. *Invest Radiol* 2015 Feb;**50**(2):67–72. https://doi.org/10.1097/RLI.0000000000000097.
11. Menys A, Helbren E, Makanyanga J, *et al.* Small bowel strictures in Crohn's disease: a quantitative investigation of intestinal motility using MR enterography. *Neurogastroenterol Motil* 2013;**25**(12):967. https://doi.org/10.1111/nmo.12229. e775.
12. Hahnemann ML, Nensa F, Kinner S, *et al.* Quantitative assessment of small bowel motility in patients with Crohn's disease using dynamic MRI. *Neurogastroenterol Motil* 2015;**27**:841–8. https://doi.org/10.1111/nmo.12558.
13. Bickelhaupt S, Froehlich JM, Cattin R, *et al.* Software-assisted small bowel motility analysis using free-breathing MRI: feasibility study. *J Magn Reson Imaging* 2014;**39**:17–23. https://doi.org/10.1002/jmri.24099.
14. Hamy V, Dikaios N, Punwani S, *et al.* Respiratory motion correction in dynamic MRI using robust data decomposition registration — application to DCE-MRI. *Med Image Anal* 2014;**18**:301–13. https://doi.org/10.1016/j.media.2013.10.016.
15. Dreja J, Ekberg O, Leander P, *et al.* Volumetric analysis of small bowel motility in an unselected cohort of patients with Crohn's disease. *Neurogastroenterol Motil* 2020;**32**(10):e13909, https://doi.org/10.1111/nmo.13909.
16. Rey D, Subsol G, Delingette H, *et al.* Automatic detection and segmentation of evolving processes in 3D medical images: application to multiple sclerosis. *Med Image Anal* 2002;**6**:163–79. https://doi.org/10.1016/S1361-8415(02)00056-7.
17. de Jonge CS, Gollifer RM, Nederveen AJ, *et al.* Dynamic MRI for bowel motility imaging—how fast and how long? *Br J Radiol* 2018;**91**(1088):20170845. https://doi.org/10.1259/bjr.20170845.
18. Fedorov A, Beichel R, Kalpathy-Cramer J, *et al.* 3D Sectionr as an image computing platform for the quantitative imaging network. *Magn Reson Imaging* 2012;**30**:1323–41. https://doi.org/10.1016/j.mri.2012.05.001.
19. Åkerman A, Månsson S, Fork FT, *et al.* Computational postprocessing quantification of small bowel motility using magnetic resonance images in clinical practice: an initial experience. *J Magn Reson Imaging* 2016;**44**:277–87. https://doi.org/10.1002/jmri.25166.
20. Gollifer RM, Menys A, Plumb A, *et al.* Automated versus subjective assessment of spatial and temporal MRI small bowel motility in Crohn's disease. *Clin Radiol* 2019;**74**:814.e9. https://doi.org/10.1016/j.crad.2019.06.016. 814.e19.
21. Horn BKP, Schunck BG. Determining optical flow. *Artif Intell* 1981;**17**:185–203. https://doi.org/10.1016/0004-3702(81)90024-2.
22. McCormick M, Liu X, Jomier J, *et al.* ITK: enabling reproducible research and open science. *Front Neuroinformatics* 2014;**8**:13. https://doi.org/10.3389/fninf.2014.00013.
23. Ronneberger O, Fischer P, Brox T. U-Net: convolutional networks for biomedical image segmentation. In: Navab N, Hornegger J, Wells W, *et al.*, editors. *Medical image computing and computer-assisted intervention – miccai 2015. Lecture notes in computer science*vol. 9351. Cham: Springer; 2015, https://doi.org/10.1007/978-3-319-24574-4_28.
24. Fidon L, Li W, Garcia-Peraza-Herrera LC, *et al.* Generalised Wasserstein Dice Score for imbalanced multi-class segmentation using holistic convolutional networks. In: Crimi A, Bakas S, Kuijf H, *et al.*, editors. *Brainlesion: glioma, multiple sclerosis, Stroke and traumatic brain injuries. BrainLes 2017. Lecture notes in computer science*vol. 10670. Cham: Springer; 2018. p. 64–76. https://doi.org/10.1007/978-3-319-75238-9_6.
25. Pei M, Wu X, Guo Y, *et al.* Small bowel motility assessment based on fully convolutional networks and long short-term memory. *Knowl-Based Syst* 2017;**121**:163–72. https://doi.org/10.1016/j.knosys.2017.01.023.
26. Wu X, Zhong M, Guo Y, *et al.* The assessment of small bowel motility with attentive deformable neural network. *Inf Sci* 2020;**508**:22–32. https://doi.org/10.1016/j.ins.2019.08.059.